

1 This paper is a non-peer reviewed preprint submitted to EarthArXiv.

2

3

4 ***serac*: a R package for ShortlivEd RAdionuclide Chronology of recent**  
5 **sediment cores**

6

7 Bruel Rosalie<sup>1,2,\*</sup> and Sabatier Pierre<sup>3</sup>

8

9 <sup>1</sup>CARTELE, Université Savoie-Mont Blanc, INRA, 74200 Thonon-les-Bains, France

10 <sup>2</sup>Rubenstein Ecosystem Science Laboratory, University of Vermont, 05401 Burlington VT, USA

11 <sup>3</sup>EDYTEM, Université Savoie-Mont Blanc, CNRS, 73370, Le Bourget du Lac, France

12 \*corresponding author: [rosaliebruel@gmail.com](mailto:rosaliebruel@gmail.com)

13

14  
15  
16  
17  
18  
19  
20  
21  
22  
23  
24  
25  
26  
27  
28  
29  
30  
31  
32  
33  
34  
35  
36  
37  
38  
39  
40  
41

Table of Contents

**1. Abstract..... 3**

**2. Introduction..... 4**

**3. Models for <sup>210</sup>Pb decay ..... 6**

**3.1. Constant Flux Constant Sedimentation ..... 6**

**3.2. Constant Rate of Supply..... 7**

**3.3. Constant Initial Concentration..... 8**

**4. R code..... 8**

**5. Case studies ..... 12**

**5.1. Lake Bourget – A classic situation with only one model (CFCS) and one instantaneous event..... 12**

**5.2. Lake Iseo – An example of a sediment sequence where the three sedimentation hypotheses could be tested. Varve counting is also available. .... 13**

**5.3. Lake Luitel – an example of sediment sequence plot versus mass depth..... 14**

**5.4. Lake Saint André – an example of sediment sequence with changes in the sedimentation rate ..... 15**

**5.5. Lake Allos – an example of a sediment sequence with instantaneous deposits .. 17**

**5.6. Pierre Blanche lagoon – An example of a sediment sequence with a surface mixed layer ..... 19**

**6. Metadata..... 20**

**7. Discussion..... 22**

**8. Acknowledgements ..... 23**

**9. Data Availability ..... 24**

**10. References..... 24**

**11. Supplementary material 1 ..... 28**

**12. Supplementary material 2 ..... 29**

## 42 **1. Abstract**

43 Short-lived radionuclides are measured in surface sediment to provide a geochronology  
44 for the past century. Age-depth models can be produced from  $^{210}\text{Pb}_{\text{ex}}$  activity-derived  
45 sedimentation rates and confirmed by  $^{137}\text{Cs}$  and  $^{241}\text{Am}$  activities that are result of fallout  
46 from nuclear weapon tests and the Chernobyl accident. Different methods of age depth  
47 modelling using such data require expertise in lake sedimentation processes.

48 Here, we present a package, *serac*, that allows the user to compute an age-depth model,  
49 output a graph and an age model as a text file, and provide metadata using the free open-  
50 source statistical software R. *serac* ensures the reproducibility of age-depth or age-mass  
51 depth models and allows testing of several  $^{210}\text{Pb}_{\text{ex}}$  models (CFCS, CIC, CRS) and  
52 sedimentation hypotheses (changes in the sedimentation rates, instantaneous deposits,  
53 varved sedimentation, etc.). Using several case studies, including lakes and lagoon in  
54 different environments, we demonstrate the use of the programme in diverse situations  
55 that may be encountered.

56 The rising number of sediment cores in recent palaeo studies and the need to correlate  
57 them require reproducible methods. *serac* is a user-friendly code that enables age model  
58 computation for the past century and encourages the standardisation of outputs.

59

60 **Keywords:** Shortlived radionuclide; R package;  $^{210}\text{Pb}$  model;  $^{137}\text{Cs}$ ; age model; metadata

61

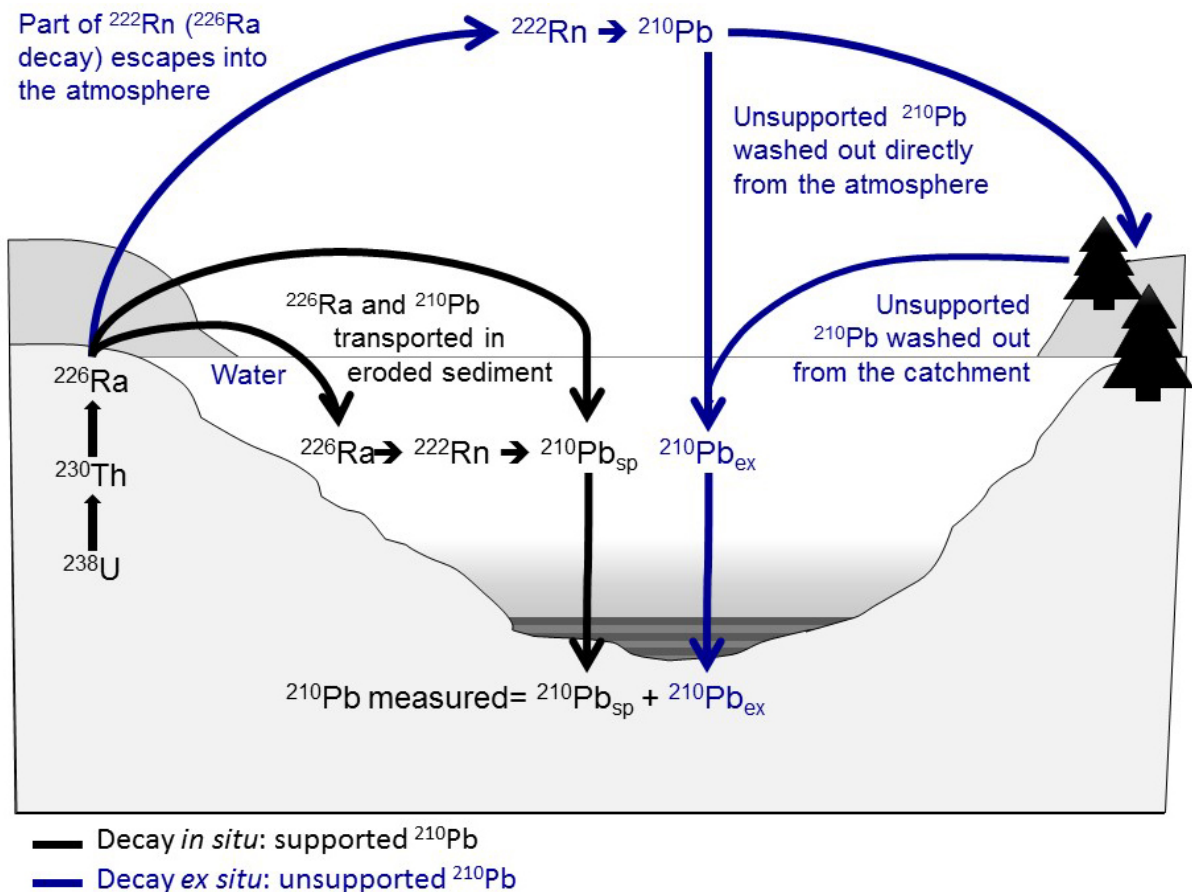
## 62 **2. Introduction**

63 Dating sediments is the first and critical step of any palaeo-study. If annual varves are  
64 absent, short-lived radionuclides provide the most accurate and widely used age-depth  
65 model technique for the past century. Accurately dating this period is crucial in  
66 palaeoclimate and palaeoecological studies because it contains many socio-ecological  
67 changes. Furthermore, there is a great amount of instrumental and historical data (e.g.,  
68 floods, constructions) for this period, and a precise age-model is needed to correlate these  
69 data to proxies. Short-lived radionuclide dating is based on measurements of the activity  
70 of  $^{137}\text{Cs}$ ,  $^{241}\text{Am}$ ,  $^{210}\text{Pb}$ , and  $^{226}\text{Ra}$ .  $^{137}\text{Cs}$  and  $^{241}\text{Am}$  can provide up to three anchoring points  
71 to constrain age-depth models from 1950 AD on. However, they only contribute to linear  
72 models, assuming that the sedimentation remained constant; however, in natural  
73 environmental contexts, sedimentation is affected by different processes (floods, river  
74 channel changes) and/or human activities (dam construction, eutrophication,  
75 agriculture). However,  $^{210}\text{Pb}$  and  $^{226}\text{Ra}$  activities can be used to reconstruct the rate of  
76 decay of the excess  $^{210}\text{Pb}$  and to infer sedimentation rates and ages.

77 Over the decade following 1955, nuclear weapons tests by the United-States, the former  
78 URSS, and the United Kingdom released nuclear by-products into the atmosphere. The  
79 isotope  $^{137}\text{Cs}$  ( $t_{1/2}= 30.15$  years) peaked in 1963, accompanied by a smaller peak in  $^{241}\text{Am}$   
80 ( $t_{1/2}= 432$  years), which results from  $^{241}\text{Pu}$  decay (one of the elements in fallout from  
81 atmospheric nuclear weapons tests). The Chernobyl accident in 1986 further dispersed  
82  $^{137}\text{Cs}$  into the atmosphere of the northern hemisphere (Appleby et al., 1991). Independent  
83 of human activities,  $^{210}\text{Pb}$  excess activity can be used to estimate environmental  
84 sedimentation dynamics.  $^{210}\text{Pb}$  is an isotope of lead that forms during the decay sequence  
85 of  $^{238}\text{U}$ . The basic methodology of  $^{210}\text{Pb}$  dating was first established in a seminal paper by  
86 Goldberg (1963).  $^{210}\text{Pb}$  comes results from the disintegration of  $^{226}\text{Ra}$  in rock, sediments  
87 and water, and from the disintegration of  $^{222}\text{Rn}$  in the atmosphere (Figure 1). While  $^{226}\text{Ra}$   
88 and  $^{210}\text{Pb}$  triggered by erosion in the watershed are in secular equilibrium ( $^{210}\text{Pb}$   
89 supported), the  $^{210}\text{Pb}$  produced in the atmosphere by  $^{222}\text{Rn}$  decay are removed from the  
90 atmosphere by dry and wet fallout and are integrated in soils, lakes and sediments (Figure  
91 1, excess  $^{210}\text{Pb}$ , referred to hereafter as  $^{210}\text{Pb}_{\text{ex}}$ ). As a consequence, it is possible to  
92 estimate the atmospheric  $^{210}\text{Pb}_{\text{ex}}$  by subtracting the total  $^{210}\text{Pb}$  by  $^{226}\text{Ra}$ . The  $^{210}\text{Pb}_{\text{ex}}$   
93 activity follows an exponential decay (characterised by its half-life  $t_{1/2}= 22.3$  years) from

94 which it is possible to calculate the sedimentation rate for the past 100 to 150 years ( $\sim 5$   
 95  $\times t_{1/2}$ ). Several models to infer ages from  $^{210}\text{Pb}_{\text{ex}}$  decay have been recently proposed  
 96 (Appleby, 2008, 2001; Appleby and Oldfield, 1992; Arias-Ortiz et al., 2018; Sanchez-  
 97 Cabeza and Ruiz-Fernández, 2012) and several limitations have been described  
 98 (Baskaran et al., 2014; Binford, 1990; Cooke et al., 2010; Kirchner, 2011). These isotopes  
 99 are also used in chronologies from corals (Andrews et al., 2009; Druffel et al., 1990; Moore  
 100 and Krishnaswami, 1972; Sabatier et al., 2012) and speleothems (Baskaran and Iliffe,  
 101 1993; Condomines and Rihs, 2006) through excess or ingrowth methods.  $^{210}\text{Pb}$  can be  
 102 detected by alpha-spectrometry determination of its daughter  $^{210}\text{Po}$  ( $t_{1/2} = 138$  d);  
 103 however,  $^{137}\text{Cs}$ ,  $^{241}\text{Am}$ ,  $^{210}\text{Pb}$ , and  $^{226}\text{Ra}$  are mostly measured together in a non-destructive  
 104 gamma-spectrometric analysis. This second method allows a direct determination of  
 105  $^{210}\text{Pb}$  supported through the  $^{226}\text{Ra}$  activity.

106



107

108 **Figure 1:  $^{210}\text{Pb}$  sources in lake or marine environments**

109

110 The method is so well established that all geochronologist teams working on recent  
 111 records confidently use it. The downside of its success is that there is a lack of information  
 112 in most published age-depth models (Blaauw, 2010), as if mentioning the method  
 113 certified the accuracy of the age model. While we are not questioning the validity of every  
 114 published model, any field benefits from reproducibility of its results (Wilkinson et al.,  
 115 2016). Establishing an age-depth model is the first step of any investigation on sediment  
 116 sequences; therefore, ensuring that the hypotheses made at this stage are transparent is  
 117 critical. Blaauw (2010) provided the *clam* R code to the palaeo-community to provide an  
 118 easy, automated, transparent, documented and adaptable environment for producing  
 119 age-models from <sup>14</sup>C sequences. Herein, we propose a systematic approach to producing  
 120 chronologies for sediment cores using short-lived radionuclides (<sup>210</sup>Pb<sub>ex</sub>, <sup>137</sup>Cs and <sup>241</sup>Am)  
 121 and different types of <sup>210</sup>Pb<sub>ex</sub> models, based on the free and open-source software R. We  
 122 first describe the different hypotheses for <sup>210</sup>Pb<sub>ex</sub> decay and the resulting models; we then  
 123 introduce the argument of the R function we developed, before applying the *serac* code to  
 124 six complex case studies. We wish our code to supplement *clam* for chronologies for the  
 125 past century.

126

## 127 **3. Models for <sup>210</sup>Pb decay**

### 128 **3.1. Constant Flux Constant Sedimentation**

129 The constant flux constant sedimentation rate (CFCS) model method is based on the  
 130 hypothesis that there is neither mixing nor Pb diffusion in the sediment (Goldberg, 1963;  
 131 Krishnaswamy et al., 1971). In a semilogarithmic diagram <sup>210</sup>Pb<sub>ex</sub> activities relative to the  
 132 depth have a linear relationship, as follows:

$$133 \quad {}^{210}\text{Pb}_{\text{ex}}^z = {}^{210}\text{Pb}_{\text{ex}}^0 \times e^{-\lambda t} \quad \text{with} \quad {}^{210}\text{Pb}_{\text{ex}} = {}^{210}\text{Pb}_{\text{mes}} - {}^{226}\text{Ra}_{\text{mes}} \text{ and } t = z/\text{SAR}$$

134 <sup>210</sup>Pb<sub>ex</sub><sup>0</sup> is the <sup>210</sup>Pb<sub>ex</sub> activity at the sediment surface (t=0), λ is the decay constant for  
 135 <sup>210</sup>Pb (Ln(2)/22,3; expressed in y<sup>-1</sup>), z is the depth and SAR is the sediment accumulation  
 136 rate expressed in (mm.yr<sup>-1</sup>). Any instantaneous event has to be removed before  
 137 computation (low <sup>210</sup>Pb<sub>ex</sub> values). If a sedimentation rate changes in time (one or two  
 138 times), it is still possible to use this model, but on each section of constant sedimentation  
 139 rate.

140 Such a model could be applied with mass depth ( $m_z$ ) instead of depth expressed in ( $\text{g}\cdot\text{cm}^{-2}$ ) and sedimentation rates are expressed as mass accumulation rates (MAR) in ( $\text{g}\cdot\text{mm}^{-2}\cdot\text{y}^{-1}$ ), as follows:

$$144 \quad m_z = \sum_{j=0}^{j=i} DBD_j \times \Delta z_j \quad \text{with} \quad DBD_j = \frac{\Delta m_j}{S \Delta z_j}$$

143 For this model we have to calculate the section dry bulk densities (DBD express in  $\text{g}\cdot\text{cm}^{-3}$ );  $\Delta z$  is the section width and  $S$  is the core cross section (in  $\text{cm}^2$ ). The CFCS model applied versus mass depth (by cluster or not) presents a very interesting alternative to CRS model (Abril, 2019; Tylmann et al., 2016).

149

### 150 **3.2.Constant Rate of Supply**

151 The constant rate of supply (CRS) model is based on the hypothesis that the flux of  $^{210}\text{Pb}_{\text{ex}}$  (P) is constant, but the SAR varies with time (Appleby and Oldfield, 1978). As a result, the  $^{210}\text{Pb}_{\text{ex}}$  activity decreases when sediment fluxes increase. This model defined the cumulative activity  $A(t)$  ( $\text{mBq}\cdot\text{cm}^{-2}$ ) during time  $t$ , corresponding to a depth  $z$ , as follows:

$$155 \quad A(t) = \int_0^t P(t) \cdot dt$$

156 The  $^{210}\text{Pb}_{\text{ex}}$  inventory can then be calculated by taking in account the decay of  $^{210}\text{Pb}_{\text{ex}}$  over time, as follows:

$$158 \quad I = P_0 \int_0^\infty e^{-\lambda t} dt = \frac{P_0}{\lambda} = \sum_{z=0}^\infty (^{210}\text{Pb})_{\text{ex}}^z m_z$$

159 where  $\sum_{z=0}^\infty (^{210}\text{Pb})_{\text{ex}}^z m_z$  represents the  $^{210}\text{Pb}_{\text{ex}}$  activity integrated over the sediment column and  $m_z$  is the dry mass depth of the measured section at  $z$  depth, express in  $\text{g}\cdot\text{cm}^{-2}$ . If the section dry masses ( $m_z$ ) are not known, but we know those of the section DBD, the mass depths  $m_z$  can be calculated as follows:

$$163 \quad m_j = DBD \times \Delta z_j$$

164 The use of this model assumes that all depths are measured (or interpolated) and that secular equilibrium is reached (i.e., no more  $^{210}\text{Pb}_{\text{ex}}$  activities are observed in the deeper sample). The age ( $t_z$ ) at the depth  $Z$  is obtained by the equation, as follows:

166

167 
$$t_z = \frac{1}{\lambda} \times \ln \left[ \frac{\sum_{z=0}^{\infty} ({}^{210}\text{Pb})_{ex}^z m_z}{\sum_{z=z}^{\infty} ({}^{210}\text{Pb})_{ex}^z m_z} \right]$$

168 where  $\sum_{z=z}^{\infty} ({}^{210}\text{Pb})_{ex}^z m_z$  represents the  ${}^{210}\text{Pb}_{ex}$  activity integrated below depth z.

169 When the CRS model is applied, a “too-old” age error described by Binford (1990) is  
 170 always present for the deeper core sections. The “too-old” age error arises from  
 171 underestimation of  ${}^{210}\text{Pb}_{ex}$  and may result from analytical limitations, sampling strategy  
 172 or both. This underestimation is that their  ${}^{210}\text{Pb}_{ex}$  ages are older than their true ages,  
 173 hence the name “too-old” age error. Thus,  ${}^{210}\text{Pb}_{ex}$  dating based on the CRS model must be  
 174 conducted with caution (Blais et al., 1995) or corrected for (Tylmann et al., 2016) to avoid  
 175 “too-old” age error for deeper core sections (Binford, 1990).

176

### 177 **3.3.Constant Initial Concentration**

178 The constant initial concentration (CIC) model is based on the hypothesis that any  
 179 changes in  ${}^{210}\text{Pb}_{ex}$  or the sedimentation rate are synchronous and reversed so that the  
 180 initial activity within the sediment remain constant (Pennington et al., 1976). The model  
 181 relies on the following equation:

182 
$$t_z = \frac{1}{\lambda} \times \ln \left[ \frac{{}^{210}\text{Pb}_{ex}^0}{{}^{210}\text{Pb}_{ex}^z} \right]$$

183 where  $t_z$  is the age at depth z,  ${}^{210}\text{Pb}_{ex}^0$  is the activity at the surface of the sediment, and  
 184  ${}^{210}\text{Pb}_{ex}^z$  is the activity at depth z. This model cannot be used if bioturbation has affected  
 185 the sediment column or if an instantaneous event perturbed the  ${}^{210}\text{Pb}_{ex}$  decrease profile  
 186 (low  ${}^{210}\text{Pb}_{ex}$  values).

187 Uncertainties in the CRS and CIC model derived ages are computed from equations from  
 188 Sanchez-Cabeza and Ruiz-Fernández, (2012).

189

## 190 **4. R code**

191 We developed a package on the open-source software R (R Core Team, 2014). All input  
 192 files must be saved in a tab separated ‘.txt’ format, with periods as decimal delimiters.  
 193 Table 1 illustrates typical data input. Depth top (depth\_min) and bottom (depth\_max)

194 represent the sampling interval of each sample. The  $^{137}\text{Cs}$ ,  $^{241}\text{Am}$ , and density columns are  
 195 optional, but the latter (density) is required for inventory calculations, CFCS mass depth  
 196 calculations and the CRS model. Even if all depths were not analysed for short-lived  
 197 radionuclides, all depths and corresponding densities are emplaced in the input file to not  
 198 extrapolate density data (NA in Table 1), which could present different patterns in regard  
 199 to their different environmental systems. If density data is not available, the analysed  
 200 depths are sufficient for age modelling (except for the CRS model). The input file must be  
 201 placed in a sub-folder of the Cores folder, e.g., *serac\Cores\MyCore\MyCore.txt* and the R  
 202 working space must be in *serac\*.

203 The function *serac\_input\_formatting('MyCore')* can be used to help format the input file.  
 204 To use it, place the raw input file (column names in first row, data starting from the second  
 205 row) in the folder as described above. This function asks the user to identify columns,  
 206 rename them, and replace the input data file automatically.

207 The package can be downloaded from the GitHub repository  
 208 <https://github.com/rosalieb/serac>, or with the package devtools (Wickham et al., 2018)  
 209 and the code:

```
210 library(devtools)
211 devtools::install_github("rosalieb/serac", build_vignettes = TRUE)
212 library(serac)
```

213

214 **Table 1. *serac* input file for an example (Lake Iseo). Units are given as an indication, but should not be included**  
 215 **in the input file to prevent any issues with file reading. \* indicates input data that are optional. NA correspond**  
 216 **to missing data: we recommend including continuous density data as  $^{210}\text{Pb}_{\text{ex}}$  can be interpolated (or depth not**  
 217 **considered) if needed, while density cannot.**

218

depth_min (mm)	depth_max (mm)	density* (g/cm3)	Pb210ex (Bq/kg)	Pbex210_er (Bq/kg)	Cs137* (Bq/kg)	Cs137_er* (Bq/kg)	Am241* (Bq/kg)	Am241_er* (Bq/kg)
0	6	0.059	370	8	18.1	0.5	0.6	0.3
6	11	0.042	414	11	25.5	0.8	0.2	0.4
11	17	0.048	381	9	26.9	0.7	0.3	0.3
17	22.5	0.065	322	11	29.9	0.8	0.2	0.35
22.5	27.5	0.074	284	7	43.7	0.8	0.6	0.3
27.5	40.5	0.063	247.5	NA	NA	NA	NA	NA
40.5	48	0.052	211	8	77.5	1	0	0
48	54	0.053	249.5	NA	NA	NA	NA	NA
54	58.5	0.054	288	9	233	1.9	0.4	0.35

58.5	64.5	0.055	232	8	631	2.7	0.27	0.4
64.5	70.5	0.069	225	NA	NA	NA	NA	NA
70.5	75	0.082	218	9	1305	5	3.307	0.7
75	83	0.055	166	6	67.1	1	0.1	0.3
83	88.5	0.079	143	NA	NA	NA	NA	NA
88.5	95	0.065	120	6	38.4	0.6	0.7	0.25
95	101	0.057	139	NA	NA	NA	NA	NA
101	111	0.048	158	7	26.7	0.6	0.26	0.26
111	119	0.049	156	NA	NA	NA	NA	NA
119	130	0.050	154	6	47.9	0.8	1.2	0.3
130	139.5	0.072	129	6	155.6	1.5	3.79	0.4
139.5	150	0.087	88	5	96	0.9	1.09	0.29
150	159.5	0.101	96	6	61.6	1	1.1	0.4
159.5	164	0.107	82	6	19.1	0.4	0.55	0.28
164	173	0.097	63	6	7.7	0.3	0.14	0.3
173	179.5	0.107	55.5	NA	NA	NA	NA	NA
179.5	187.5	0.117	48	5	2.4	0.2	0.3	0.3
187.5	199.5	0.107	47	NA	NA	NA	NA	NA
199.5	209	0.106	46	3	0.7	0.1	0.2	0.16
209	234	0.107	40	NA	NA	NA	NA	NA
234	244.5	0.108	34	5	0.5	0.1	0	0
244.5	254	0.107	34	NA	NA	NA	NA	NA
254	264	0.105	34	5	0.23	0.14	0	0
264	283.5	0.108	31	NA	NA	NA	NA	NA
283.5	295	0.110	28	3	0.7	0.1	0	0
295	305	0.110	23	NA	NA	NA	NA	NA
305	317	0.109	18	4	0.19	0.13	0	0

219

220 **The code includes the sedimentation hypotheses described in the previous section (CFCS, CRS, and CIC). The**  
221 **only requested arguments are the name of the core (must be the same of the folder and the data input) and the**  
222 **coring year. All other arguments have default values and do not have to be filled on the first run. Some**  
223 **arguments are logical (i.e., TRUE or FALSE), other are entered in the form of vectors (e.g., list of sedimentation**  
224 **hypotheses, upper and lower limits for instantaneous deposits). All depths must be entered in millimetres.**

225 Table 2 summarises the main options; the case studies included in the next section  
226 showcase different scenarios. A 'cheat sheet' summarising the steps and main functions  
227 is available in Supplementary Materials 1.

228

229 **Table 2. Main options included in *serac*. Refer to Supplementary Material 2 for complete list of functions.**

Category	Description
Site ID	<b>Only two arguments are mandatory to run the code: the name of the core and the coring year. Other arguments have default values that can be used.</b> The name of the core has to match the folder name and the file name with the input data.

$^{210}\text{Pb}_{\text{ex}}$	The user can choose to plot $^{210}\text{Pb}_{\text{ex}}$ measurements, with or without potential instantaneous deposits. One of the three models can be visualised. The choice to include or not include instantaneous deposits will automatically remove the corresponding measurements.
$^{137}\text{Cs}$	The user can choose to plot $^{137}\text{Cs}$ , and if so, to identify Chernobyl, the fallouts from nuclear war tests, and the firsts fallouts (logical arguments).
$^{241}\text{Am}$	The user can choose to plot $^{241}\text{Am}$ and identify the fallouts from nuclear war tests
Model	List of model(s) the user wants to test. Choice among CFCS, CRS, CIC.
Photo	A photo of the sediment sequence can be added, upon precision of the upper and lower limit of the core (in mm). The photo will be automatically cropped.
Instantaneous deposit	Instantaneous deposits (flood, earthquake, slump layers) that should be excised can be added with this argument.
Ignore	For several reason, the user may want to ignore a measurement that is not part of an instantaneous deposit. This can be managed with this argument.
Sedimentation change	Up to two changes in the sedimentation rate can be tested. The depths of the changes are added in a vector.
Plot options	The user can choose whether to export the age-depth model figure using logical arguments. Colours and character size can also be modified.
Historic events	Historical events (e.g., flood, construction of a dam...) can be plotted on the last window.
Supplementary descriptor(s)	Up to two supplementary descriptors can be plotted. If done, an additional input file with these data should be included in the working folder.
Varves	Varve counting can be added on the age-depth model plot. If done, an additional input file with depths (in mm) and corresponding years must be included in the working folder.
Surface Mixed Layer	A depth in mm above which the sediment is considered to be mixed.
Mass depth	Logical (TRUE/FALSE) argument, to decide whether radionuclides should be plotted against mass accumulated depth. Default entries for sediment changes ignore instantaneous deposits and surface mixed layers, are in mm. Another argument (input_depth_mm) allows these depths to be entered in $\text{g.cm}^{-2}$ when turned to FALSE.

## 231 5. Case studies

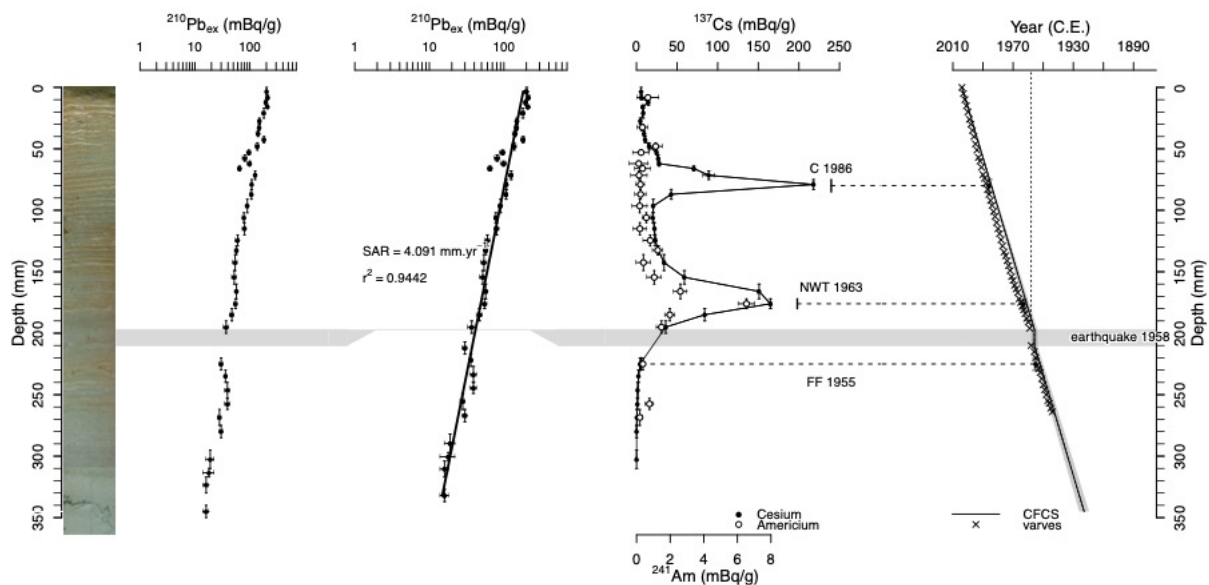
### 232 5.1. Lake Bourget – A classic situation with only one model (CFCS) and one 233 instantaneous event

234 Lake Bourget (45°44.7420N, 5°51.6850E) is a large lowland hard-water lake in the  
235 Northern French Alps, 18 km long and 2.8 km wide. This core was sampled in the deepest  
236 part of the lake at 145 m water depth and records of recent eutrophication (Giguet-Covex  
237 et al., 2010). Using *serac*, it is possible to calculate SAR = 3.849 mm.y<sup>-1</sup> from short-lived  
238 radionuclides data on this core and provide age modelling at a higher resolution than the  
239 initial stepout (determined by *stepout*, e.g., 1 mm in the example below). The example  
240 below includes <sup>210</sup>Pb<sub>ex</sub> CFCS models, <sup>137</sup>Cs and <sup>241</sup>Am peaks, varve counting with the  
241 identification of an instantaneous deposit linked to a historical earthquake (Figure 2) with  
242 the following arguments:

```
243 serac(name="LDB", coring_yr=2004, model=c("CFCS"), plotphoto=TRUE, minphoto=c(0),  
244 maxphoto=c(370), plot_Pb=T, plot_Pb_inst_deposit=T, plot_Cs=T, plot_Am=T, Cher=c(75,85  
245 ), Hemisphere=c("NH"), NWT=c(172,180), FF=c(220,230), inst_deposit=c(197,210), histori  
246 c_d=c(197,210), historic_a=c(1958), historic_n=c("earthquake  
247 1958"), varves=T, plotpdf=T, stepout=1)
```

248

249 Details on the several arguments are available in Supplementary Material 1.



250

251 **Figure 2. Age model derived from the *serac* function with, from left to right: core photo,  $^{210}\text{Pb}_{\text{ex}}$ ,  $^{210}\text{Pb}_{\text{ex}}$**   
252 **corrected of instantaneous deposits,  $^{137}\text{Cs}$  and  $^{241}\text{Am}$  activities and the CFCS age model with varve counting,**  
253  **$^{137}\text{Cs}$  and  $^{241}\text{Am}$  peaks and the identification of the 1958 earthquake**

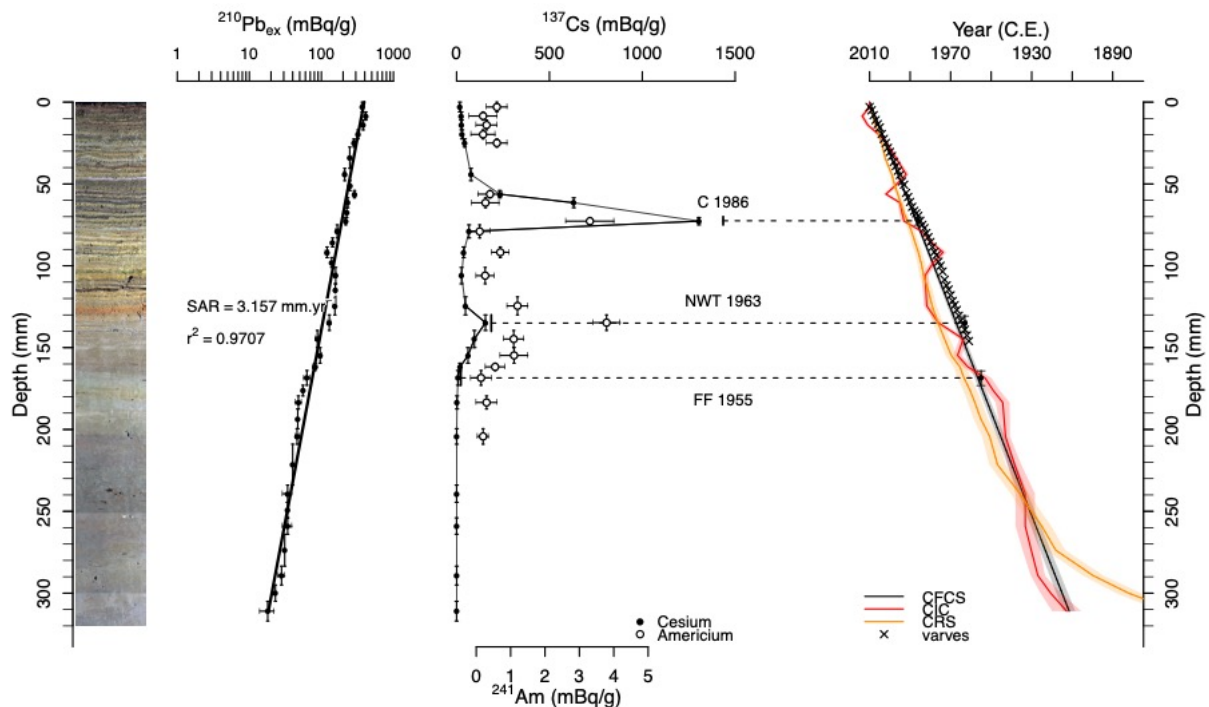
254 **5.2. *Lake Iseo* – An example of a sediment sequence where the three**  
255 **sedimentation hypotheses could be tested. Varve counting is also**  
256 **available.**

257 Lake Iseo ( $45^{\circ}44.205'\text{N}$ ;  $10^{\circ}4.340'\text{E}$ ) is a large lowland lake in Northern Italy 25 km long  
258 and  $60.9 \text{ km}^2$  in surface area. This core is a sample from the Monte Isola plateau at  
259 approximately 70 m depth and contains evidence for a recent eutrophication (Rapuc et  
260 al., 2018). From short-lived radionuclides data on this core (Table 1),  $\text{SAR} = 3.157 \text{ mm.y}^{-1}$ .  
261 In the script below, note that we request to visualise all three  $^{210}\text{Pb}_{\text{ex}}$  models,  $^{137}\text{Cs}$  and  
262  $^{241}\text{Am}$  peaks and varve counting (Figure 3) and we use a 5 mm resolution for our  
263 interpolated model.

```
264 serac(name="Iseo",coring_yr=2010,model=c("CFCS","CIC","CRS"),plotphoto=TRUE,minp  
265 hoto=c(0),maxphoto=c(320),plot_Pb=T,plot_Am=T,plot_Cs=T,Cher=c(70,75),Hemispher  
266 e=c("NH"),NWT=c(130,140),FF=c(164,173),varves=TRUE,plotpdf=T,stepout=5)
```

267

268 The comparison between varve counting, artificial radionuclides and the  $^{210}\text{Pb}_{\text{ex}}$  model  
269 shows that the CFCS model is preferable for this core and that there is evidence for the  
270 “too-old” age error described first by Binford (1990) for the CRS model in the deeper core  
271 sections and now widely observed (Abril, 2019; Tylmann et al., 2016, 2013). The “too-old”  
272 age error arises from an underestimation of  $^{210}\text{Pb}_{\text{ex}}$  in deeper core sections in relation to  
273 analytical limitations, sampling strategy or both.



274

275 **Figure 3. Age model derived from the *serac* function, from left to right: core photo,  $^{210}\text{Pb}_{\text{ex}}$ ,  $^{137}\text{Cs}$  and  $^{241}\text{Am}$**   
 276 **activities and age model (CFCs, CIC, CRS) with varve counting and  $^{137}\text{Cs}$  and  $^{241}\text{Am}$  peaks.**

277

### 278 **5.3.Lake Luitel – an example of sediment sequence plot versus mass depth**

279 Lake Luitel (FR) is a very small system (1.94 ha) located 1262 m above sea level, in a  
 280 depression within the crystalline Belledonne range bedrock (Western Alps). The lake  
 281 colour is black, typical of organic rich water and is encircled by bog type vegetation. An  
 282 80-cm-long core (LUI12P1) was collected from the deeper part of the lake (6 m) in 2012  
 283 to reconstruct the history of multiple industrial and urban mercury (Hg) emissions  
 284 (Guédron et al., 2016).

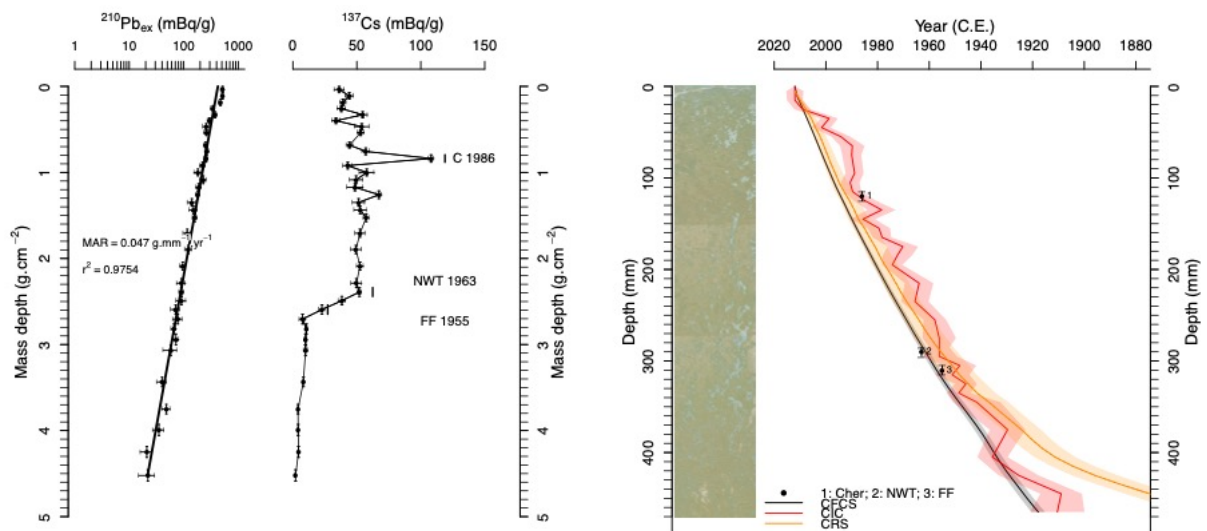
285 This lake is rich in organic matter and thus presents a large amount of poral water; the  
 286 classic CFCs model does not match the  $^{137}\text{Cs}$  fallouts well (note that  $^{241}\text{Am}$  was under the  
 287 detection limit and is thus not presented in Figure 4). In such a lake system, a  
 288 semilogarithmic plot of  $^{210}\text{Pb}_{\text{ex}}$  activities versus mass depth allows us to consider density  
 289 variations in regard to sediment compaction (Abril, 2019; Tylmann et al., 2016). We thus  
 290 plot the CRS, CIC and CFCs models based on the mass depth model (Figure 4). The MAR is  
 291 well defined ( $0.047 \text{ g}\cdot\text{mm}^{-1}\cdot\text{y}^{-1}$ ,  $r^2=0.975$ ) and the age model is in good agreement with the  
 292 1955 and 1963 AD  $^{137}\text{Cs}$  markers and at lesser extent with the Chernobyl fallout. The CRS  
 293 model also provides a reliably good age model in regards to the  $^{137}\text{Cs}$  data, but still present

294 too old ages for the deeper samples. The CIC model displays several ages inversions,  
 295 which we want to avoid. The best age modelling is done thanks to *serac* and includes the  
 296 CFCS mass depth calculation with the following arguments:

```
297 serac(name="LUI", coring_yr=2012, model=c("CFCS", "CIC", "CRS"), mass_depth=T, plotphoto=
298 T, minphoto=c(0), maxphoto=c(470), plot_Pb=T, plot_Cs=T, Cher=c(115,125), Hemisphere=c("NH"),
299 NWT=c(285,295), FF=c(305,315), plotpdf=TRUE)
```

300

301 Note that the  $^{137}\text{Cs}$  peaks (or other depth-related arguments) could be identified in the  
 302 *serac* function in mm by default or in  $\text{g}\cdot\text{cm}^{-2}$  if we add the argument *input\_depth\_mm = F*.



303

304 **Figure 4.** From left to right:  $^{210}\text{Pb}_{\text{ex}}$  activities,  $^{137}\text{Cs}$  activities, photo of the core, and the age models  
 305 (CFCS\_mass\_depth, CRS, CIC) for the Lake Luitel sediment core. Note that in the left and central parts, data are  
 306 plotted versus mass depth, while in the right part, data are plotted versus depth.

307

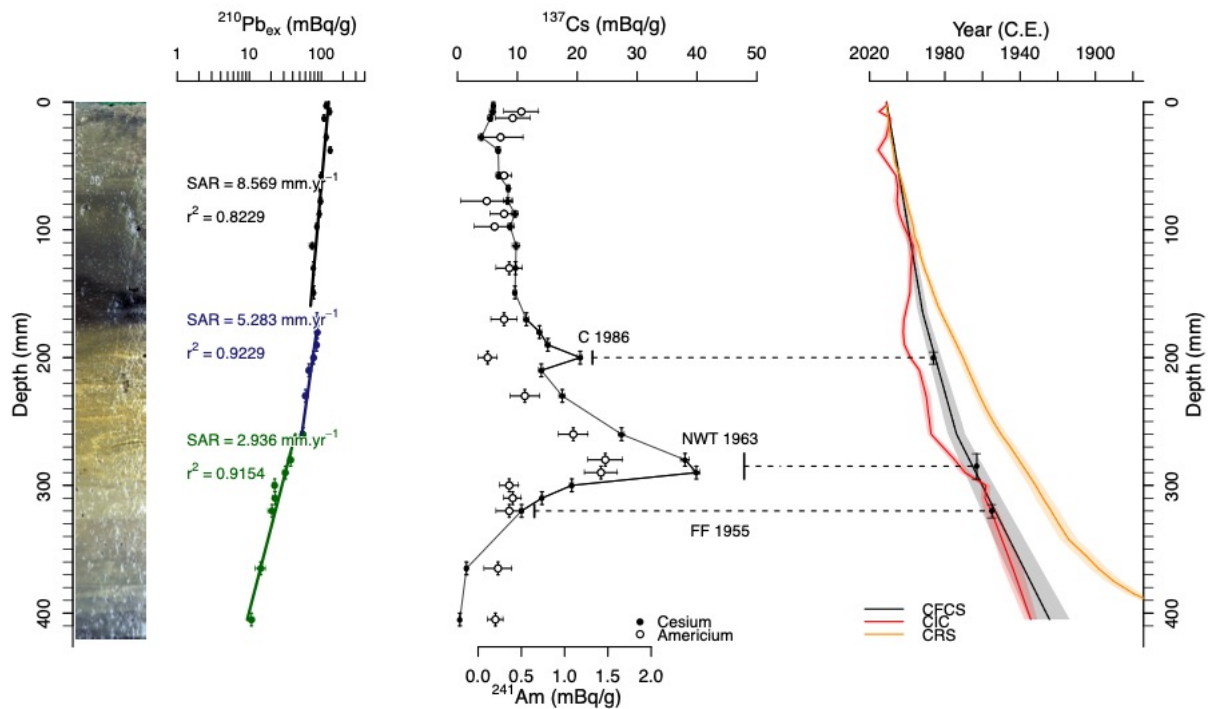
#### 308 **5.4. Lake Saint André – an example of sediment sequence with changes in** 309 **the sedimentation rate**

310 Lake Saint André (FR) is a relatively small system (7.64 ha), formed in 1248 after a large  
 311 landside. Vineyards have occupied approximately 36% of its 48.5 ha watershed since the  
 312 beginning of World War II. A 1-m core (SAN11P2) was collected from the deepest part of  
 313 Lake Saint André (12 m) in 2011 to investigate long-term succession and the diffuse  
 314 transfer of herbicides, fungicides, and insecticide treatments (Sabatier et al., 2014).

315 A logarithmic plot of  $^{210}\text{Pb}_{\text{ex}}$  activity (Figure 5) shows a general decrease with three  
316 distinct linear trends. According to the (CFCS) model applied to each part of the profile,  
317 we can define mean accumulation rates of  $2.9 \pm 0.2 \text{ mm.y}^{-1}$  between depths of 41 and 26  
318 cm,  $5.3 \pm 0.6 \text{ mm.y}^{-1}$  between 26 and 16.5 cm, and  $8.6 \pm 1.3 \text{ mm.y}^{-1}$  in the upper 16.5 cm  
319 of the core (3).  $^{137}\text{Cs}$  and  $^{241}\text{Am}$  activities (3) are in good agreement with the ages derived  
320 from the  $^{210}\text{Pb}_{\text{ex}}$ -CFCS model and support the interpretation of two primary  
321 sedimentation rate changes in  $\sim 1973 \pm 5 \text{ y}$  and  $1994 \pm 2.5 \text{ y}$ . These two changes in the  
322 sedimentation rate are related to vineyard practices increasing erosion in the watershed  
323 during two periods: (1) in the early 1970s, with the local use of heavy farm machinery  
324 and (2) in the early 1990s, with increasing applications of postemergence herbicides  
325 (Glyphosate, see Sabatier et al., 2014 for more details). The age modelling conducted  
326 through *serac*, including the two changes in sedimentation rate, takes the following  
327 arguments:

```
328 serac(name="SAN",coring_yr=2011,model=c("CFCS","CIC","CRS"),plotphoto=TRUE,minp  
329 hoto=c(0),maxphoto=c(420),plot_Pb=T,sedchange=c(165,260),plot_Am=T,plot_Cs=T,Ch  
330 er=c(195,205),Hemisphere=c("NH"),NWT=c(275,295),FF=c(315,325),plotpdf=TRUE,arc  
331 hive_metadata=T)
```

332



333

334 **Figure 5. From left to right: photography,  $^{210}\text{Pb}_{\text{ex}}$  activity,  $^{137}\text{Cs}$  and  $^{241}\text{Am}$  activities, and the age model (CFCS,**  
 335 **CRS, CIC) for the Lake Saint André sediment core.**

336

337 **5.5. Lake Allos – an example of a sediment sequence with instantaneous**  
 338 **deposits**

339 Lake Allos is a high-altitude lake in the French Alps (2230 m a.s.l., 0.6 km<sup>2</sup>). Half of the 5-  
 340 km<sup>2</sup> catchment is drained by three permanent torrents that transport terrigenous flows  
 341 towards the lake mainly during extreme precipitation events (Wilhelm et al., 2015, 2012).  
 342 A plot of  $^{210}\text{Pb}_{\text{ex}}$  activity (Figure 6) shows a general decrease with low activities at several  
 343 depths that correspond to graded beds. To illustrate these sedimentary events, we add  
 344 one to two supplementary descriptors (*suppdSCRIPTOR*) to the age model figure, such as  
 345 geochemical data (XRF). Ca enrichment associated with coarser grain size evidence four  
 346 instantaneous deposits in the Allos sediment sequence, indicating a large input from the  
 347 watershed, while Fe content is associated with continuous sedimentation (Figure 6, see  
 348 Wilhelm et al., 2012 for more details). As these events are instantaneous, there are  
 349 removed before computing the CFCS model, which assumes a linear sedimentation rate.  
 350 In this case,  $^{210}\text{Pb}_{\text{ex}}$  activities, corrected for instantaneous deposits, show a change in the  
 351 mean sedimentation rate at 71 mm. The final age model is supported by the  $^{137}\text{Cs}$  and  
 352  $^{241}\text{Am}$  activities and by historical floods that correspond to these four instantaneous

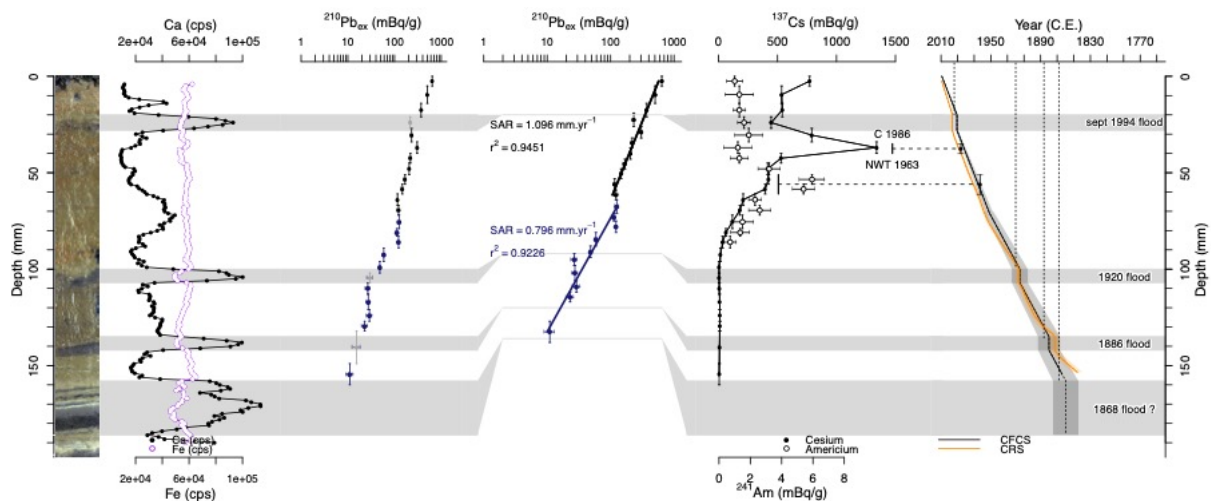
353 events. These floods deposits are also added in Figure 6 to validate the chronology. The  
 354 age modelling is conducted through *serac* and includes the historical events and one  
 355 change in sedimentation rate with the following arguments:

```
356 serac(name="ALO09P12", coring_yr=2009, model=c("CFCS", "CRS"), plotphoto=TRUE, min
357 photo=c(0), maxphoto=c(210), plot_Pb=T, plot_Pb_inst_deposit=T, inst_deposit=c(20,28,1
358 00,107,135,142,158,186), sedchange=c(71), plot_Am=T, plot_Cs=T, Cher=c(35,40), Hemisp
359 here=c("NH"), NWT=c(51,61), suppdescriptor=TRUE, descriptor_lab=c("Ca (cps)", "Fe
360 (cps)"), historic_d=c(20,28,100,107,135,142,158,186), historic_a=c(1994,1920,1886,186
361 8), historic_n=c("sept 1994 flood", "1920 flood", "1886 flood", "1868 flood ?"),
362 min_yr=c(1750), dmax=c(180), plotpdf=TRUE)
```

363

364 Note that for larges figures as Figure 6, R may sometimes not create the preview (and  
 365 gives an error) because the plotting window is too narrow. The user can try to extend the  
 366 plotting zone (which is easy in RStudio, RStudio Team, 2016). We added a logical  
 367 argument, *preview*, which can be turned to FALSE to address this issue; in this case, the  
 368 preview is simply not displayed. If the argument *plotpdf* is left to its default value, i.e.,  
 369 TRUE, the figure will still be created in the core subfolder.

370



371

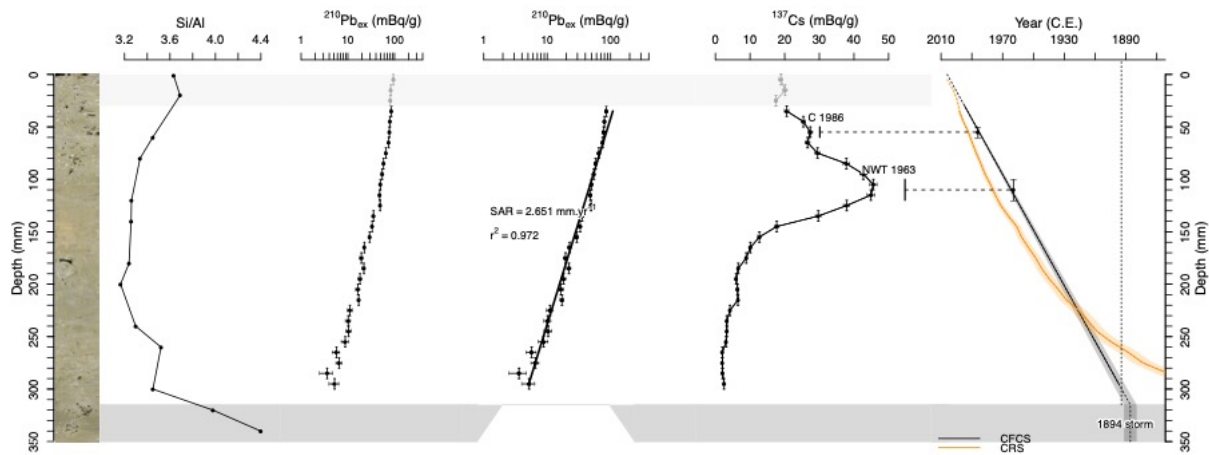
372 **Figure 6.** From left to right: core photograph, Ca/Fe ratio and raw Fe,  $^{210}\text{Pb}_{\text{ex}}$  activity with and without instantaneous  
 373 deposit events,  $^{137}\text{Cs}$  activity and  $^{241}\text{Am}$  activity, and the age model for the Lake Allos sequence. The horizontal grey  
 374 lines indicate layers that were identified as instantaneous events.

375

376 **5.6. Pierre Blanche lagoon – An example of a sediment sequence with a**  
377 **surface mixed layer**

378 The PB06 core (7.9 m) was collected in the Pierre Blanche Lagoon (PBL), in the southern  
379 part of the Palavasian lagoonal complex (France) in 2006 (Sabatier et al., 2010b). This  
380 coastal shallow water environment contains many organisms that induce bioturbation,  
381 with advection-diffusion in the upper first centimetres in the deepest regions caused by  
382 mollusc and gallery-diffusion by worms (François et al., 2002). This second process is  
383 difficult to identify and to correct for (Sabatier et al., 2010a). The resolution of the  
384 advection-diffusion model (Sharma et al., 1987) by Lecroart *et al.* (2007) applied to  $^{210}\text{Pb}_{\text{ex}}$   
385 allows the estimation of SARs and the biodiffusion coefficient ( $D_b$ ). We can thus define a  
386 surface mixed layer (SML) within which  $^{210}\text{Pb}_{\text{ex}}$  activities are perturbed; PB06 has almost  
387 constant activities in the first 3 cm (Figure 7). The  $^{210}\text{Pb}_{\text{ex}}$  activities profile is thus  
388 composed of a bioturbated upper part, characterised by a combination of sedimentation  
389 and bioturbation (SAR,  $D_b$ ) and below which a non-perturbed profile exists where  $D_b = 0$ .  
390 To solve this model, we can calculate a mean sedimentation rate for the non-bioturbated  
391 part and if we suppose that the sedimentation rate remains constant, we can extrapolate  
392 this estimate to the upper part. With *serac* we must define the SML to calculate  
393 sedimentation and create a CFCS age model. It is not possible to apply the CIC model in  
394 this case because the initial activity is perturbed. The age model for PB06 is also  
395 constrained by the  $^{137}\text{Cs}$  peaks and a historical storm event identified by geochemical data  
396 (Figure 7); for more details see Sabatier et al. (2010c). The age modelling is conducted  
397 using *serac* and includes the SML with the following arguments:

```
398 serac(name="PB06", coring_yr=2006, model=c("CFCS", "CRS"), plotphoto=TRUE, minphoto  
399 =c(0), maxphoto=c(350), plot_Pb=T, plot_Pb_inst_deposit=T, inst_deposit=c(315,350), SML  
400 =30, plot_Cs=T, Cher=c(50,60), Hemisphere=c("NH"), NWT=c(100,120), suppdescriptor=T,  
401 descriptor_lab=c("Si/Al"), historic_d=c(315,350), historic_a=c(1893), historic_n=c("1894  
402 storm"), min_yr=1870, dmax=c(350), plotpdf=TRUE)
```



403

404 **Figure 7.** From left to right: core photograph, Si/Al content,  $^{210}\text{Pb}_{\text{ex}}$  activities,  $^{137}\text{Cs}$  activities, and the age model (CFCS  
 405 and CRS).

406 The comparison among historical events (storms), artificial radionuclides and the  $^{210}\text{Pb}_{\text{ex}}$   
 407 model results in the CFCS model being preferable to the CRS for this core and evidence of  
 408 the “too-old” age error described by Binford (1990) for the CRS model in the deeper core  
 409 sections, resulting from the 1894 storm event.

410

## 411 6. Metadata

412 Every time the code is run, a metadata file is automatically generated in the folder. The  
 413 metadata file summarises the main decisions made by the user (e.g., presence/absence of  
 414 instantaneous deposit, type of model chosen) but also other general information on the  
 415 user (ORCID, affiliation, email) and the core (ISGN: International Geo Sample Number  
 416 (IGSN)/System for Earth Sample Registration Database ([www.geosamples.org](http://www.geosamples.org),  
 417 measurement laboratory, measurement method, date of measurement). These data are  
 418 entered independently from the exploration phase of the model through the function  
 419 `user_infos()` and `core_metadata()`. The former function theoretically needs to be used only  
 420 once by each new user the first time the library *serac* is used. The new user will be  
 421 required to answer several questions (affiliation, ORCID number, etc.). These information  
 422 are then integrated into the metadata file associated with the age modelling, in text  
 423 format. The `core_metadata()` function ask more details about the core itself and the  
 424 analytical data, summarised in Table 2 and will be enter according to the following lines:

425

`core_metadata(name="Mycore")`

426 These data can also be directly implemented during the age modelling phase by adding  
 427 `archive_metadata=T` in the *serac* function. The metadata listed in Table 3 emerges from  
 428 both data reports of radioactivity detections from the CNRS in France (Centre National de  
 429 la Recherche Scientifique) and a recent international survey (literature review and  
 430 questionnaire) about  $^{210}\text{Pb}$  metadata (Courtney Mustaphi et al., 2019). The French  
 431 initiative coordinated the development of a common way to present short-lived  
 432 radionuclides data through the ROZA (Rétro-observatoire Archives sédimentaires des  
 433 Zones Ateliers) experience and produced a document guiding the information needed to  
 434 store data in a repository. The review by Courtney Mustaphi et al. (2019) also suggests a  
 435 set of minimum reporting guidelines for  $^{210}\text{Pb}$  metadata and data needed to improve data  
 436 archiving standards to facilitate data reutilisation.

437 **Table 3. Example of metadata associated with the SAN core (Sabatier et al., 2014)**

Parameters	Example
ISGN	EDYSAN001
sample date	2011-12-01
coring coordinates y	45.494980
coring coordinates x	5.985720
coring method	gravity corer
laboratory subsampling method	calibrated volumetric sampler
measurement laboratory	LSM/EDYTEM, FR
instrument type	well-type germanium detector
measurement startdate	2012-01-15
measurement enddate	2012-04-05
additional comments	$^{210}\text{Pb}$ background reached

438

439 These two functions and all parameters inside are optional but we encourage the users to  
 440 use these functionalities as they help generate a more exhaustive background for the core.

441 Note that another text file is automatically generated and incremented with all new tests.  
 442 The file is found in the core folder (`~\Cores\MyCore\serac_model_history_MyCore.txt`).  
 443 It (1) provides a history of attempts and (2) displays a message in R if a code has been  
 444 tested previously. A vigilant user can then compare and trace back the logical thinking  
 445 that led to the final model.

446

## 447 **7. Discussion**

448 *serac* provides a rapid yet exhaustive tool for testing sedimentation hypotheses and  
449 creating age models for the last century. Several functions (Table 4) guide the user in  
450 building age-depth models for a given core. To choose the best chronology for the studied  
451 archives, *serac* allows different age models to be compared versus depth or mass depth  
452 with other independent markers such as artificial radionuclides fallout or historic events.  
453  $^{210}\text{Pb}_{\text{ex}}$  models are sometime used incorrectly. For instance, if the CIC model is used for a  
454 core that has instantaneous deposits with lower  $^{210}\text{Pb}_{\text{ex}}$  activities or a surface mixed layer  
455 linked to bioturbation processes; or if the CRS model is used when the  $^{210}\text{Pb}_{\text{ex}}$  inventory  
456 is not the total (activities were not measured until secular equilibrium existed between  
457  $^{210}\text{Pb}$  and  $^{226}\text{Ra}$ ). With *serac*, the sedimentation hypotheses have to be satisfied and if they  
458 are not tested, an error message will be automatically provided, explaining why. In that  
459 respect, *serac* is also a pedagogic tool. Using *serac* easily allows reproducibility of the main  
460 hypotheses behind any age-depth model (such as changes in sedimentation rates or the  
461 presence of instantaneous deposits). We believe that the availability of a user-friendly  
462 code on an open source platform to visualise and test sedimentation hypotheses is an  
463 important step towards reproducibility. *serac* allows users customisation of parameters  
464 to include, as well as cross-platform support (Windows, Linux, Macs).

465 Furthermore, if the density is present in the input data, *serac* generates the  $^{210}\text{Pb}$  and  $^{137}\text{Cs}$   
466 inventories of sediment cores, which provides the opportunity to compare these values  
467 between sites to map radionuclide fallouts. For instance,  $^{137}\text{Cs}$  inventories of Lake Iseo  
468 (1390 Bq.m<sup>-2</sup>; range: 1380-1403 Bq.m<sup>-2</sup>) and Lake Bourget (975 Bq.m<sup>-2</sup>; range: 953-997  
469 Bq.m<sup>-2</sup>) reported the same age of 2020, but present significant differences related to the  
470 higher Chernobyl accident fallout in Italy relative to that in France. The R code of *serac*  
471 can be understood relatively easily and could be adapted to fit user preferences. Output  
472 files (age model, metadata, figure) could be used (1) in the current form or integrated in  
473 a larger age model such as *clam* (2) to create a figure for publication and (3) in data saving  
474 platforms with general information on data, metadata, the age modeller, and the age  
475 model parameters, which would allow data tractability and reproducibility. It is hoped  
476 that *serac* could help the palaeoscience community standardise and enhance future age  
477 depth models that use short-lived radionuclides and allow the extension of the data  
478 lifecycle (Wilkinson et al., 2016).

479

480 **Table 4. Summary of the functions around *serac*, for a core named 'MyCore'.**

Function	Use	Output
<code>user_infos()</code>	New users run this function once to enter professional details	A .txt file in the <code>~\Cores</code> folder with user's metadata
<code>core_metadata(name = 'MyCore')</code>	Before running <i>serac</i> , but once a folder 'MyCore' had been created in the <code>~\Cores</code> folder, this function questions the user on metadata specifically related to the core (see Table 3 for details)	A <code>serac_metadata_suppmetadata.txt</code> file in the <code>~\Cores\MyCore</code> folder This supplementary data will be included to the general metadata after each model computation.
<code>serac_input_formatting(name = 'MyCore')</code>	Input data file can be formatted outside R. This function can help correct several errors (columns names, unit for depth, density calculation, etc.)	Replace <code>MyCore.txt</code> in the <code>~\Cores\MyCore</code> folder by a correctly formatted file and save the raw data in the same folder under the name <code>MyCore_raw.txt</code>
<code>serac(name = 'MyCore', coring_year = 2019)</code>	<b>Main age-depth model computation function.</b> <b>Refer to</b> Table 2 and case studies	Generate a plot in the <code>~\Cores\MyCore</code> folder (if <code>plotpdf=TRUE</code> ), a metadata file, and depth-age correspondence (raw and interpolated, according to resolution chosen by the <i>stepout</i> argument) for each type of model selected in the <i>model</i> argument.
<code>serac_map()</code>	<i>Function not describe in this paper – if GPS coordinates are given for the different cores (through the <code>core_metadata()</code> function), <code>serac_map()</code> will generate a map with the location of the different sites around the world</i>	A world map with the location of the different study sites

481

482

483 **8. Acknowledgements**

484 We thank A.-L. Develle and W. Rapuc for beta testing previous versions of *serac* and C.  
485 Pignol for recommendations on metadata outputs through the ROZA (Rétro-observatoire  
486 Archives sédimentaires des Zones Ateliers) experience at the CNRS (Centre National de  
487 Recherche Scientifique français).

## 489 9. Data Availability

490 Data to reproduce the example for Lake Allos (Figure 6) are accessible through the  
491 package.

492

## 493 10. References

- 494 Abril, J.M., 2019. Radiometric dating of recent sediments: On the performance of  $^{210}\text{Pb}$ -  
495 based CRS chronologies under varying rates of supply. *Quaternary Geochronology*  
496 51, 1–14. <https://doi.org/10.1016/j.quageo.2018.12.003>
- 497 Andrews, A., Stone, R., Lundstrom, C., DeVogelaere, A., 2009. Growth rate and age  
498 determination of bamboo corals from the northeastern Pacific Ocean using refined  
499  $^{210}\text{Pb}$  dating. *Marine Ecology Progress Series* 397, 173–185.  
500 <https://doi.org/10.3354/meps08193>
- 501 Appleby, P.G., 2008. Three decades of dating recent sediments by fallout radionuclides: a  
502 review. *The Holocene* 18, 83–93. <https://doi.org/10.1177/0959683607085598>
- 503 Appleby, P.G., 2001. Chronostratigraphic Techniques in Recent Sediments, in: Last, W.M.,  
504 Smol, J.P. (Eds.), *Tracking Environmental Change Using Lake Sediments, Basin*  
505 *Analysis, Coring, and Chronological Techniques. Developments in*  
506 *Paleoenvironmental Research Series*. Dordrecht, pp. 171–203.
- 507 Appleby, P.G., Oldfield, F., 1992. Applications of lead-210 to sedimentation studies, in:  
508 *Uranium-Series Disequilibrium: Applications to Earth, Marine, and Environmental*  
509 *Sciences*. Clarendon Press ; Oxford University Press, Oxford : Oxford ; New York.
- 510 Appleby, P.G., Oldfield, F., 1978. The calculation of lead-210 dates assuming a constant  
511 rate of supply of unsupported  $^{210}\text{Pb}$  to the sediment. *CATENA* 5, 1–8.  
512 [https://doi.org/10.1016/S0341-8162\(78\)80002-2](https://doi.org/10.1016/S0341-8162(78)80002-2)
- 513 Appleby, P.G., Richardson, N., Nolan, P.J., 1991.  $^{241}\text{Am}$  dating of lake sediments.  
514 *Hydrobiologia* 214, 35–42. <https://doi.org/10.1007/BF00050929>
- 515 Arias-Ortiz, A., Masqué, P., Garcia-Orellana, J., Serrano, O., Mazarrasa, I., Marbà, N.,  
516 Lovelock, C.E., Lavery, P., Duarte, C.M., 2018. Reviews and syntheses:  $^{210}\text{Pb}$ -derived  
517 sediment and carbon accumulation rates in vegetated coastal ecosystems: setting  
518 the record straight. *Biogeosciences Discussions* 1–47.  
519 <https://doi.org/10.5194/bg-2018-78>
- 520 Baskaran, M., Iliffe, T.M., 1993. Age determination of recent cave deposits using excess  $^{210}$   
521  $\text{Pb}$  - A new technique. *Geophysical Research Letters* 20, 603–606.  
522 <https://doi.org/10.1029/93GL00531>
- 523 Baskaran, M., Nix, J., Kuyper, C., Karunakara, N., 2014. Problems with the dating of  
524 sediment core using excess  $^{210}\text{Pb}$  in a freshwater system impacted by large scale  
525 watershed changes. *Journal of Environmental Radioactivity* 138, 355–363.  
526 <https://doi.org/10.1016/j.jenvrad.2014.07.006>
- 527 Binford, M.W., 1990. Calculation and uncertainty analysis of  $^{210}\text{Pb}$  dates for PIRLA project  
528 lake sediment cores. *J Paleolimnol* 3, 253–267.

529 Blaauw, M., 2010. Methods and code for 'classical' age-modelling of radiocarbon  
530 sequences. *Quat. Geochronol.* 5, 512–518.  
531 <https://doi.org/10.1016/j.quageo.2010.01.002>

532 Blais, J.M., Kalff, J., Cornett, R.J., Evans, R.D., 1995. Evaluation of  $^{210}\text{Pb}$  dating in lake  
533 sediments using stable Pb, Ambrosia pollen, and  $^{137}\text{Cs}$ . *J. Paleolimnol.* 13, 169–178.

534 Condomines, M., Rihs, S., 2006. First  $^{226}\text{Ra}$ – $^{210}\text{Pb}$  dating of a young speleothem. *Earth  
535 and Planetary Science Letters* 250, 4–10.  
536 <https://doi.org/10.1016/j.epsl.2006.06.012>

537 Cooke, C.A., Hobbs, W.O., Michelutti, N., Wolfe, A.P., 2010. Reliance on  $^{210}\text{Pb}$  Chronology  
538 Can Compromise the Inference of Preindustrial Hg Flux to Lake Sediments.  
539 *Environmental Science & Technology* 44, 1998–2003.  
540 <https://doi.org/10.1021/es9027925>

541 Courtney Mustaphi, C.J., Brahney, J., Aquino-López, M.A., Goring, S., Orton, K., Noronha, A.,  
542 Czaplewski, J., Asena, Q., Paton, S.C., Panga Brushworth, J., 2019. Guidelines for  
543 reporting and archiving  $^{210}\text{Pb}$  sediment chronologies to improve fidelity and  
544 extend data lifecycle. *Quat. Geochronol.* 52, 77–87.

545 Druffel, E.R.M., King, L.L., Belastock, R.A., Buesseler, K.O., 1990. Growth rate of a deep-sea  
546 coral using  $^{210}\text{Pb}$  and other isotopes. *Geochimica et Cosmochimica Acta* 54, 1493–  
547 1499. [https://doi.org/10.1016/0016-7037\(90\)90174-J](https://doi.org/10.1016/0016-7037(90)90174-J)

548 François, F., Gerino, M., Stora, G., Durbec, J.-P., Poggiale, J.-C., 2002. Functional approach to  
549 sediment reworking by gallery-forming macrobenthic organisms: modeling and  
550 application with the polychaete *Nereis diversicolor*. *Marine Ecology Progress  
551 Series* 229, 127–136. <https://doi.org/10.3354/meps229127>

552 Giguet-Covex, C., Arnaud, F., Poulenard, J., Enters, D., Reyss, J.-L., Millet, L., Lazzaroto, J.,  
553 Vidal, O., 2010. Sedimentological and geochemical records of past trophic state and  
554 hypolimnetic anoxia in large, hard-water Lake Bourget, French Alps. *J. Paleolimnol.*  
555 43, 171–190. <https://doi.org/10.1007/s10933-009-9324-9>

556 Goldberg, E.D., 1963. Geochronology with  $^{210}\text{Pb}$  in radioactive dating. *International  
557 Atomic Energy Contribution* 1510, 121–131.

558 Guédron, S., Amouroux, D., Sabatier, P., Desplanque, C., Develle, A.-L., Barre, J., Feng, C.,  
559 Guiter, F., Arnaud, F., Reyss, J.L., Charlet, L., 2016. A hundred year record of  
560 industrial and urban development in French Alps combining Hg accumulation  
561 rates and isotope composition in sediment archives from Lake Luitel. *Chemical  
562 Geology* 431, 10–19. <https://doi.org/10.1016/j.chemgeo.2016.03.016>

563 Kirchner, G., 2011.  $^{210}\text{Pb}$  as a tool for establishing sediment chronologies: examples of  
564 potentials and limitations of conventional dating models. *Journal of Environmental  
565 Radioactivity* 102, 490–494. <https://doi.org/10.1016/j.jenvrad.2010.11.010>

566 Krishnaswamy, S., Lal, D., Martin, J.M., Meybeck, M., 1971. Geochronology of lake  
567 sediments. *Earth Planet. Sci. Lett.* 11, 407–414. [https://doi.org/10.1016/0012-821X\(71\)90202-0](https://doi.org/10.1016/0012-821X(71)90202-0)

568

569 Lecroart, P., Schmidt, S., Anschutz, P., Jouanneau, J.-M., 2007. Modeling sensitivity of  
570 biodiffusion coefficient to seasonal bioturbation. *Journal of Marine Research* 65,  
571 417–440. <https://doi.org/10.1357/002224007781567630>

572 Moore, W.S., Krishnaswami, S., 1972. Coral growth rates using  $^{228}\text{Ra}$  and  $^{210}\text{Pb}$ . *Earth and  
573 Planetary Science Letters* 15, 187–190. [https://doi.org/10.1016/0012-821X\(72\)90059-3](https://doi.org/10.1016/0012-821X(72)90059-3)

574

575 Pennington, W., Cambray, R.S., Eakins, J.D., Harkness, D.D., 1976. Radionuclide dating of  
576 the recent sediments of Blelham Tarn. *Freshw. Biol.* 6, 317–331.  
577 <https://doi.org/10.1111/j.1365-2427.1976.tb01617.x>

578 R Core Team, 2014. R: A language and environment for statistical computing. R  
579 Foundation for Statistical Computing, Vienna, Austria.

580 Rapuc, W., Sabatier, P., Andrič, M., Crouzet, C., Arnaud, F., Chapron, E., Šmuc, A., Develle,  
581 A.-L., Wilhelm, B., Demory, F., Reyss, J.-L., Régnier, E., Daut, G., Von Grafenstein, U.,  
582 2018. 6600 years of earthquake record in the Julian Alps (Lake Bohinj, Slovenia).  
583 *Sedimentology* 65, 1777–1799. <https://doi.org/10.1111/sed.12446>

584 RStudio Team, 2016. RStudio: Integrated Development for R. RStudio, Inc., Boston, MA.

585 Sabatier, P., Dezileau, L., Barbier, M., Raynal, O., Lofi, J., Briquieu, L., Condomines, M.,  
586 Bouchette, F., Certain, R., Grafenstein, U.V., Jorda, C., Blanchemanche, P., 2010a.  
587 Late-Holocene evolution of a coastal lagoon in the Gulf of Lions (South of France).  
588 *Bulletin de la Société Géologique de France* 181, 27–36.  
589 <https://doi.org/10.2113/gssgfbull.181.1.27>

590 Sabatier, P., Dezileau, L., Blanchemanche, P., Siani, G., Condomines, M., Bentaleb, I., Piquès,  
591 G., 2010b. Holocene Variations of Radiocarbon Reservoir Ages in a Mediterranean  
592 Lagoonal System. *Radiocarbon* 52, 91–102.

593 Sabatier, P., Dezileau, L., Briquieu, L., Colin, C., Siani, G., 2010c. Clay minerals and  
594 geochemistry record from northwest Mediterranean coastal lagoon sequence:  
595 Implications for paleostorm reconstruction. *Sedimentary Geology* 228, 205–217.  
596 <https://doi.org/10.1016/j.sedgeo.2010.04.012>

597 Sabatier, P., Poulenard, J., Fanget, B., Reyss, J.-L., Develle, A.-L., Wilhelm, B., Ployon, E.,  
598 Pignol, C., Naffrechoux, E., Dorioz, J.-M., Montuelle, B., Arnaud, F., 2014. Long-term  
599 relationships among pesticide applications, mobility, and soil erosion in a vineyard  
600 watershed. *Proc. Natl. Acad. Sci.* 111, 15647–15652.  
601 <https://doi.org/10.1073/pnas.1411512111>

602 Sabatier, P., Reyss, J.-L., Hall-Spencer, J.M., Colin, C., Frank, N., Tisnérat-Laborde, N.,  
603 Bordier, L., Douville, E., 2012.  $^{210}\text{Pb}$  and  $^{226}\text{Ra}$  chronology reveals rapid growth rate of  
604 *Madrepora oculata* and *Lophelia pertusa* on  
605 world's largest cold-water coral reef. *Biogeosciences* 9, 1253–1265.  
606 <https://doi.org/10.5194/bg-9-1253-2012>

607 Sanchez-Cabeza, J.A., Ruiz-Fernández, A.C., 2012.  $^{210}\text{Pb}$  sediment radiochronology: An  
608 integrated formulation and classification of dating models. *Geochimica et*  
609 *Cosmochimica Acta, Environmental Records of Anthropogenic Impacts* 82, 183–  
610 200. <https://doi.org/10.1016/j.gca.2010.12.024>

611 Sharma, P., Gardner, L.R., Moore, W.S., Bollinger, M.S., 1987. Sedimentation and  
612 bioturbation in a salt marsh as revealed by  $^{210}\text{Pb}$ ,  $^{137}\text{Cs}$ , and  $^7\text{Be}$  studies:  
613 Sedimentation and bioturbation. *Limnol. Oceanogr.* 32, 313–326.  
614 <https://doi.org/10.4319/lo.1987.32.2.0313>

615 Tylmann, W., Bonk, A., Goslar, T., Wulf, S., Grosjean, M., 2016. Calibrating  $^{210}\text{Pb}$  dating  
616 results with varve chronology and independent chronostratigraphic markers:  
617 Problems and implications. *Quat. Geochronol.* 32, 1–10.

618 Tylmann, W., Enters, D., Kinder, M., Moska, P., Ohlendorf, C., Poręba, G., Zolitschka, B.,  
619 2013. Multiple dating of varved sediments from Lake Łazduny, northern Poland:  
620 Toward an improved chronology for the last 150 years. *Quaternary Geochronology*  
621 15, 98–107. <https://doi.org/10.1016/j.quageo.2012.10.001>

622 Wickham, H., Hester, J., Chang, W., RStudio, R), R.C. team (Some namespace and vignette  
623 code extracted from base, 2018. devtools: Tools to Make Developing R Packages  
624 Easier.  
625

626 Wilhelm, B., Arnaud, F., Sabatier, P., Crouzet, C., Brisset, E., Chaumillon, E., Disnar, J.-R.,  
627 Guiter, F., Malet, E., Reyss, J.-L., Tachikawa, K., Bard, E., Delannoy, J.-J., 2012. 1400  
628 years of extreme precipitation patterns over the Mediterranean French Alps and  
629 possible forcing mechanisms. *Quat. Res.* 78, 1–12.

630 Wilhelm, B., Sabatier, P., Arnaud, F., 2015. Is a regional flood signal reproducible from lake  
631 sediments? *Sedimentology* 62, 1103–1117. <https://doi.org/10.1111/sed.12180>

632 Wilkinson, M.D., Dumontier, M., Aalbersberg, I.J., Appleton, G., Axton, M., Baak, A.,  
633 Blomberg, N., Boiten, J.-W., da Silva Santos, L.B., Bourne, P.E., Bouwman, J., Brookes,  
634 A.J., Clark, T., Crosas, M., Dillo, I., Dumon, O., Edmunds, S., Evelo, C.T., Finkers, R.,  
635 Gonzalez-Beltran, A., Gray, A.J.G., Groth, P., Goble, C., Grethe, J.S., Heringa, J., 't Hoen,  
636 P.A.C., Hooft, R., Kuhn, T., Kok, R., Kok, J., Lusher, S.J., Martone, M.E., Mons, A.,  
637 Packer, A.L., Persson, B., Rocca-Serra, P., Roos, M., van Schaik, R., Sansone, S.-A.,  
638 Schultes, E., Sengstag, T., Slater, T., Strawn, G., Swertz, M.A., Thompson, M., van der  
639 Lei, J., van Mulligen, E., Velterop, J., Waagmeester, A., Wittenburg, P., Wolstencroft,  
640 K., Zhao, J., Mons, B., 2016. The FAIR Guiding Principles for scientific data  
641 management and stewardship. *Scientific Data* 3, 160018.  
642 <https://doi.org/10.1038/sdata.2016.18>  
643

serac cheat sheet



1

Using the library devtools, install serac: `devtools::install_github("rosalieb/serac", build_vignettes = TRUE)`  
**Step 1** User information – optional, fill it only once or when your affiliation / details change `user_infos()`

2

**Step 2.1** Core analysis

1. Photo.
2. XRF core scanner – potential supplementary descriptors.
3. Sediment characterization: granulometry, wet weight, LOI, density – potential supplementary descriptors.
4. Radionuclides measurements.

**Step 2.2** Prepare the input files  
**For a given core named "MyCore", user should have in a given working directory "MyWD":**

```
~/MyWD/Cores/MyCore/...
MyCore.txt*           — radionuclides data
MyCore.jpg           — core photo
MyCore_varves.txt     — varves
MyCore_proxy.txt     — additional proxies
(* means mandatory, txt files with tab separators)
```

**Function below helps editing the MyCore.txt file:**  
`serac_input_formatting(name="MyCore")`

**MyCore.txt should have the following column names and units:**

Column name	Description (unit)
depth_top	alt. name: depth_min (mm)
depth_bottom	alt. name: depth_max (mm)
density	(g.cm <sup>-3</sup> )
Pbex	Unsupported Lead 210 excess (Bq.kg <sup>-1</sup> )
Pbex_er	Error <sup>210</sup> Pb <sub>ex</sub> (Bq.kg <sup>-1</sup> )
Cs	Cesium 137 (Bq.kg <sup>-1</sup> )
Cs_er	Error <sup>137</sup> Cs (Bq.kg <sup>-1</sup> )
Am	Americium 241 (Bq.kg <sup>-1</sup> )
Am_er	<sup>241</sup> Am (Bq.kg <sup>-1</sup> )

**Optional: enter metadata for this core**  
`core_metadata(name="MyCore")`

**Step 2.3** Model computation

**List of arguments included in the main function:**  
`args(serac)`

```
?serac
serac(name, coring_yr, model, Cher, NWT, Hemisphere, FF,
inst_deposit, input_depth_mm, ignore, mass_depth, plotpdf,
preview, plotphoto, minphoto, maxphoto, Pbc01,
inst_depositcol, modelcol, historic_d, historic_a,
historic_n, historic_test, suppdessor, descriptor_lab,
plot_Am, plot_Cs, plot_Pb, plot_Pb_inst_deposit,
plot_CFCS_regression, varves, dmin, dmax, sedchange,
min_yr, SML, stepout, mycex, archive_metadata, save_code)
```

**MAKE SURE YOUR WORKING DIRECTORY IS THE GOOD ONE (i.e., the one with the 'Cores' folder)**  
`getwd() ; setwd("~/MyWD")`

**Compute model:**  
`Modell <- serac(name="MyCore", coring_year=2019)`

**A list is created - explore this object with the following functions:**  
`class(Modell)`  
`[1] list`  
`names(Modell)`  
`[1] Output depends on which model was selected`

**Step 2.4** Compare output with prior knowledge (from step 2.1)

<p>Low fit OR potential changes in sedimentation rate OR potential instantaneous deposit OR warning messages that could be addressed</p> <p style="text-align: center;">↓</p> <p>Go back to step 2.3 and edit code</p>	<p>Best model, good agreement between <sup>210</sup>Pb<sub>ex</sub>, <sup>137</sup>Cs, and historical events, all changes in sedimentation rate or wet weight/density have been addressed</p> <p style="text-align: center;">↓</p> <p>Done!</p>
--	---

3

**Step 3** Understand the output files  
 Running serac created some files in the ~/MyWD/Cores/MyCore/ folder.

File	What it is
serac_model_history_MyCore.txt	History of the code combination you tried.
serac_metadata_suppmetadata.txt	File created with the function "core_metadata("MyCore")". Fill it in once when you get the core, then carry on with model tests.
MyCore.pdf	If plotpdf=TRUE (default), the model is automatically generated in the folder.
MyCore_Metadata_YYYY-MM-DD.txt	Metadata and output regarding the model you computed. A file you would typically share with your colleagues, or include as Appendix to a manuscript submission.
MyCore_CFCS.txt (.csv) MyCore_CFCS_interpolation.txt (.csv)	Dated depth if CFCS model was chosen, and interpolated model with intervals determined by stepout (default to 5 mm).
MyCore_CIC.txt (.csv) MyCore_CIC_interpolation.txt (.csv)	Dated depth if CIC model was chosen, and interpolated model with intervals determined by stepout (default to 5 mm).
MyCore_CRS.txt (.csv) MyCore_CRS_interpolation.txt (.csv)	Dated depth if CRS model was chosen, and interpolated model with intervals determined by stepout (default to 5 mm).

646 **12. Supplementary material 2**

Argument	Default	Description
Name	Mandatory argument e.g., name=" ALO09P12"	Name of the core, given using quotes. Defaults to the core provided with serac. Use preferably the published name of the core for traceability.
coring_yr	Mandatory argument e.g., coring_yr=2009	Coring year
model	model=c("CFCS")	Select 1 to 3 item between c("CFCS", "CIC", "CRS"). If several models are selected, they will all be plotted together in the last window.
Cher	Cher=NA	If $^{137}\text{Cs}$ measurement were done, where do you detect the Chernobyl peak? The argument is a vector of two depth given in millimetres giving the top and bottom threshold for the 1986 Chernobyl event. The user can run the model without giving any specification before making a decision. In such case, leave the argument empty.
NWT	NWT=NA	If $^{137}\text{Cs}$ measurement were done, where do you detect the Nuclear Weapon Test peak? The argument is a vector of two depth given in millimetres giving the top and

		bottom threshold for the 1960s Nuclear Weapon Test event. The user can run the model without giving any specification before making a decision. In such case, leave the argument empty.
Hemisphere	Hemisphere=NA	Choose between North Hemisphere "NH" and South Hemisphere "SH" depending on the location of your system. This argument is required if you choose to plot NWT, as the age of the maximum fallout varies with the Hemisphere considered (Northern hemisphere: 1963; Southern hemisphere: 1965)
FF	FF=NA	If <sup>137</sup> Cs measurement were conducted, where do you detect the First Fallout period? The argument is a vector of two depths given in millimetres giving the top and bottom threshold for the First Fallout period in 1955. The user can run the model without giving any specification before making a decision. In such case, leave the argument empty.
inst_deposit	inst_deposit=c(0)	Upper and lower depths (in mm) of sections of abrupt accumulation that inst_deposit c() should be excised, e.g., c(100, 120,

		185, 195) for two sections of 10.0-12.0 cm and 18.5-19.5 cm depth
mass_depth	mass_depth=FALSE	Logical (TRUE/FALSE) argument, to decide whether radionuclides should be plotted against mass accumulated depth.
ignore	ignore=c()	The depth (in mm) of any sample that should be ignored from the age-depth model computation, e.g., c(55) will remove the measurement done at 55 mm (between 50 and 60 mm). The data will be plotted by default in grey on the output graph (you can change this with the inst_depositcol argument)
input_depth_m m	input_depth_mm=TRUE	Logical argument to indicate the unit of the entry depth (when user detects instantaneous deposits, Cher, NWT and FF peaks, points to ignore, or SML). By default (TRUE), entry depths in mm. If FALSE, entry depths are in g.cm-2 and are then converted in the function to allow the rest of the code to run.
Plotpdf	plotpdf=FALSE	Logical argument to indicate whether you want the output graph to be saved in pdf format to your folder.

Preview	preview=TRUE	Logical argument to indicate whether you want the output graph to be plotted. Default is TRUE, and the graph is plotted within your R session. It might be convenient to turn this argument to FALSE if errors telling you that your R window is too small continue to appear.
plotphoto	plotphoto=FALSE	Logical argument to indicate whether you want to plot the photo of the core along your age-model. If plotphoto=TRUE, you need to indicate the upper and lower limit of the photo in mm in following arguments. An additional jpg file with the photo should be included in the folder with the initial data.
Minphoto	minphoto=c()	Mandatory if plotphoto=TRUE. Lower limit of the core photo in mm, e.g., minphoto=c(0) indicates that the photo starts at 0 mm. The photo will automatically be truncated according to the minimum depth of the age model given in other arguments.
Maxphoto	maxphoto=c()	Mandatory if plotphoto=TRUE. Upper limit of the core photo in mm, e.g., maxphoto=c(320) indicates that the photo ends at 32 cm. The photo will

		automatically be truncated according to the maximum depth of the age model given in other arguments.
Pbcol	Pbcol=c("black","midnightblue","darkgreen")	Vector of colour to plot $^{210}\text{Pb}_{\text{ex}}$ data. If length(Pbcol)>1, the different colours will be used to plot the different slopes between change(s) in sedimentation rate. Example of colour vector: Pbcol=c("black","midnightblue","darkgreen").
inst_depositcol	inst_depositcol=grey(0.85)	The colour to plot the data points within an instantaneous deposit or ignored data. Example: inst_depositcol=grey(0.85).
modelcol	modelcol=c("black","red","darkorange")	Vector of colour to plot a different model if length(model)>1. If length(modelcol)>1, the different colours will be used to plot the different changes in sedimentation rate. Example of colour vector: modelcol=c("black","red","darkorange") to plot "CFCS", "CIC", "CRS" models in this order.
historic_d	historic_d=c()	Vector with upper and lower depths of the historical event(s), e.g., historic_d=c(120,130,220,250) will identify the event between

		both 12 and 13 cm and 22 and 25 cm on the last window of the age model.
historic_a	historic_a=c()	Vector of years of different historical events, e.g., historic_a=c(1970,1895) will add two points at 1970 and 1895 on the last window of the age model. Historical events can be older than the dated section, in which case the depth is obtained from the model if historic_d is not specified. historic_a is a vector twice as short as historic_d, as each age corresponds to an upper+lower limit in the vector 'historic_d'. If not all ages are known, put NA in the vector, e.g., historic_a=c(NA,1895)
historic_n	historic_n=c()	Vector of names of different historical events, e.g., historic_n=c("1970 flood","1895 flood"). Optional. If you plot several events and do not want to plot all the names, add an NA in the vector, e.g., historic_n=c(NA,"1895 flood") will understand that the first event does not have a name, but the second does.

suppdescrpto r	suppdescrptor=FALSE	Up to two supplementary descriptor(s) to plot in an additional window. Logical argument. The decision on plotting more than one supplementary descriptor depends on the length of the vector descriptor_lab. An additional input file with these data should be included in the folder with the initial data.
descriptor_lab	descriptor_lab=c()	Label used on the axis, e.g., descriptor_lab=c("LOI", "Ca/Fe") if two supplementary descriptors are specified.
suppdescrpto rcol	suppdescrptorcol=c("black","purple")	Vector of colours to plot different descriptors if length(descriptor_lab)>1. If length(descriptor_lab)>1, the different colours will be used to plot the different changes in the sedimentation rate. Example of colour vector: suppdescrptorcol=c("black","purple").
plot_Am	plot_Am=FALSE	Logical argument indicating whether or not serac should plot <sup>241</sup> Am.

plot_Cs	plot_Cs=FALSE	Logical argument indicating whether or not serac should plot $^{137}\text{Cs}$ .
plot_Pb	plot_Pb=TRUE	Logical argument indicating whether or not serac should plot $^{210}\text{Pb}_{\text{ex}}$ .
plot_Pb_inst_deposit	plot_Pb_inst_deposit=FALSE	Logical argument indicating whether or not serac should plot $^{210}\text{Pb}_{\text{ex}}$ without instantaneous deposits. If TRUE, inst_deposit should not be a null vector.
varves	varves=FALSE	Logical argument to indicate whether varve counting results should be plotted on the last window. An additional input file with these data should be included in the folder with the initial data.
dmin	dmin=c()	Minimum depth of the age-depth model (useful if the user does not want to plot the upper part).
dmax	dmax=c()	Maximum depth of age-depth model (useful if the user does not want to plot the lower part or wants to plot data below the extent of the radionuclides data). dmax cannot be in the middle of an instantaneous deposit. For example, if there is an instantaneous deposit between 180 and 200 mm, dmax cannot be

		190 mm and will be automatically converted to 200 mm.
sedchange	sedchange=c(0)	Up to two changes in sedimentation rate, e.g., sedchange=c(175,290) indicates two changes of sedimentation rate at 17.5 and 29.0 cm.
min_yr	min_yr=1880	The minimum year limit for the age-depth model plot. The user can adjust this argument after a first computation of the model.
SML	SML=c(0)	Surface Mixed Layer: a depth in mm above which the sediment is considered to be mixed. For example, SML=30 indicates that the first 3 cm are mixed sediment: the data points are plotted but not included in the CFCS models.
stepout	stepout=1	Depth resolution for the file output in mm.
mycex	mycex=1	Graphical parameter: a multiplication factor to increase (mycex>1) or decrease (mycex<1) label sizes.
Historic_test	Historic_test=c()	Vector of years of different historical events, e.g., historic_test=c(1970). Visualisation tool for known ages. This argument will plot a vertical line in the last window. Can be

		useful when the user knows specific ages of historical events and wants to fit the model with this event.
archive_metadata	archive_metadata=FALSE	Logical argument. If TRUE, require fields regarding the measurements on the core. Allows missing information; just press 'ENTER' in your computer (leave an empty field)
save_code	save_code=TRUE	Logical argument. If TRUE (default), the code is saved in the output object. If serac is within a Shiny app, the history cannot be easily extracted, so it is convenient to be able to turn it to FALSE

647